Seventh Canadian Masonry Symposium
McMaster University
Hamilton, Ontario
June 4-7, 1995

THE FLEXURAL DESIGN OF POST-TENSIONED HOLLOW CLAY MASONRY

Kelvin J. Graham[1] and Adrian W. Page[2]

ABSTRACT

Prestressed single skin clay or concrete hollow masonry is being used in Australia for the construction of low rise buildings in high wind areas to enhance its flexural performance. The level of prestress controls the cracking and the serviceability performance of the masonry, and the ultimate strength is governed by its cracked section performance. This paper presents the results of a fundamental study of the flexural behaviour of post-tensioned hollow clay masonry. The study consisted of a series of flexural tests on wallettes with a parallel analytical investigation of the flexural behaviour at both the serviceability and ultimate strength limit states. The variables included the level of prestress, the reinforcement ratio of the section, the degree of restraint of the tendons within the cores of the masonry, and the influence of the grout on the composite behaviour of the cross section.

INTRODUCTION

Unreinforced masonry typically has a low tensile strength which is directly influenced by the bond between the mortar and the masonry unit. Because of this low tensile strength, its flexural performance is considerably restricted unless its capacity can be enhanced by some form of reinforcing or prestressing. Prestressed single skin clay or concrete hollow masonry is now being used in Australia for the construction of low rise buildings in high wind areas. The level of prestress controls the degree of cracking and the serviceability performance, and the ultimate strength is enhanced by the fact that the masonry acts as a reinforced section.

Although the principles of prestressed concrete design are well established and widely

1 Postgraduate Student, Department of Civil Engineering and Surveying, The University of Newcastle, NSW, 2308, Australia

2 CBPI Professor in Structural Clay Brickwork, Department of Civil Engineering and Surveying, The University of Newcastle, NSW, 2308, Australia

accepted, prestressed masonry is much less common and under researched. Important fundamental research on prestressed masonry has been carried out by Phipps (Phipps, 1993) and some previous tests have been performed on post–tensioned hollow concrete masonry walls. This and other research has been recently summarised (Graham, 1995). Review papers have also been produced (Schultz and Scolforo, 1992; 1992) and design principles for post–tensioned masonry recently presented (Hendry, 1991). No comprehensive study has been carried out for Australian applications.

This paper describes a fundamental study of the flexural behaviour of post–tensioned hollow clay masonry. The study consisted of a series of flexural tests on wallettes with a parallel analytical investigation of the flexural behaviour at both serviceability and ultimate strength limit states. Some of the tests have been reported previously (Graham and Page, 1994). The variables considered included the level of prestress, the reinforcement ratio of the section, the degree of restraint of the tendon within the cores of the masonry and the influence of grout (i.e., bonded or unbonded construction).

EXPERIMENTAL PROGRAMME

Test Specimens

A total of 26 walls were tested. The walls were constructed from hollow clay blocks (310 mm (length) × 76 mm (height) × 150 mm (width)) and a 1:1:6 mortar (cement:lime:sand by volume). The walls were laid in running bond and face–shell bedded throughout (face–shell width 33 mm). Each wall panel was 20 courses high and 2.5 units long, resulting in overall dimensions of 1700 mm (height) × 800 mm (width). One prestressing rod was centrally located in the central core of each panel. Stack bonded prisms were constructed for each mortar batch to allow the masonry compressive strength and the flexural bond strength of the joints to be determined (using a bond wrench). The masonry had a mean compressive strength of 15.6 MPa and a mean flexural bond strength of 0.21 MPa.

When the walls were at an age of greater than 28 days they were post–tensioned. The prestress was induced by stressing the steel rod in the central core. Two bar types were used: a 16 mm diameter conventional Y16 deformed bar (400 MPa nominal yield strength); and a 20 mm diameter TL20 "Threadlock" bar (nominal yield strength 500 MPa). This latter bar is produced with deformations which can also double as a thread, so that the rod can be readily joined or anchored using appropriate couplers.

Two different bar sizes were used to produce different reinforcement ratios, resulting in ultimate behaviour which ranged from under–reinforced to over–reinforced. The prestress was applied by a hydraulic jack through an extended end block to allow access to the rod so that the steel strain could be monitored. The prestressing load was monitored with a load cell during jacking. Immediate anchorage losses could therefore be eliminated during the jacking process. Resistance gauges were also glued to the rods at mid length to monitor the steel strains during the test. A separate investigation was carried out to determine the typical deferred losses for this particular type of masonry (Graham, 1995).

One of the important practical variables is the restraint of the prestressing rod in the core of the hollow masonry units as this has a direct influence on ultimate behaviour. Three conditions were investigated: the core containing the rod was fully grouted after stressing ("Grouted" (GR)) (see Table 1); the core was left ungrouted but the rod restrained by clay brick inserts pre–glued in some of the hollow units to prevent any transverse movement of

Table 1. Summary of Test Results

Wallette	Bar Type	Effective Prestress Level (MPa)	Results		
			Cracking Moment (kN/m)	Ultimate Moment (kN/m)	Failure Mode
1F–GR	Y16	0.0	1.16	4.86	U/R
2F–GR	Y16	1.11	3.33	5.72	U/R
3F–GR	TL20	0.0	1.29	9.62	O/R
4F–GR	TL20	1.0	3.35	9.93	Bal
5F–G	Y16	0.0	0.5	4.84	O/R
6F–G	Y16	0.93	3.33	5.57	U/R
7F–G	TL20	0.0	0.95	7.99	O/R
8F–G	TL20	0.98	3.25	8.87	O/R
9F–G	TL20	2.03	6.11	9.51	O/R
15F–G	TL20	0.96	3.78	7.66	O/R
10F–UG	Y16	0.0	0.86	2.29	O/R
11F–UG	Y16	1.04	3.25	4.29	Bal
12F–UG	TL20	0.0	0.52	2.96	O/R
13F–UG	TL20	0.95	2.83	4.44	O/R
14F–UG	TL20	1.94	5.21	6.59	O/R
1S–GR	Y16	0.0	1.85	5.89	U/R
2S–GR	Y16	1.0*	3.39	6.44	U/R
3S–GR	TL20	0.0	1.38	7.87	O/R
4S–GR	TL20	1.0*	3.52	10.04	O/R
5S–G	Y16	0.94	3.69	5.91	U/R
6S–G	TL20	0.99	4.15	9.50	O/R
7S–G	TL20	1.91	6.42	10.47	O/R
8S–UG	Y16	0.97	3.96	4.83	Bal
9S–UG	TL20	0.99	3.66	4.98	O/R
10S–UG	TL20	1.93	6.17	7.72	O/R
11S–UG	TL20	–	2.13	5.13	O/R

F Indicates a "flexure" test or four point loading arrangement
S Indicates a "shear" test or three point loading arrangement
* Nominal values of prestress level because the strain gauges were affected by the grout
– Premature failure caused by sudden impact loading due to a failure in the loading system

the rod during testing ("Guided" (G)) (see Table 1); and the rod was left unrestrained in the core ("Unguided" (UG)). For the grouted cases the mean compressive strength of the grout was 10.1 MPa.

Three levels of prestress were considered: zero; 1 MPa; and 2 MPa, with the imposed force in the rod being chosen accordingly. The main influence of the level of prestress is on the cracking behaviour of the masonry, rather than the ultimate strength. A summary of the properties of the 26 walls tested is given in Table 1.

Flexural Tests

All walls were tested in the horizontal plane with appropriate corrections for dead load effects. Two types of flexural tests were performed: a conventional four point bending test to yield a zone of constant moment in the central region of the span (referred to as a "flexure" test); and a three point bending test with the applied load located near one end of

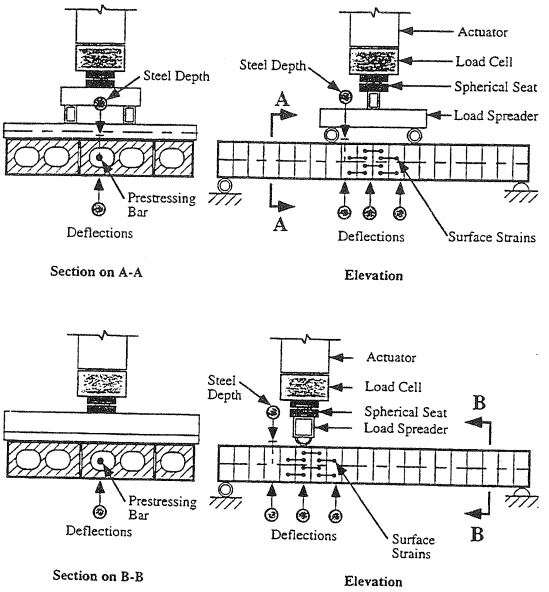

Figure 1. Testing Arrangement

the span to maximise the shear force on the section (referred to as a "shear" test). A schematic arrangement of the two tests is shown in Figure 1. The load was applied under displacement control to allow better control of the post–cracking behaviour.

During each test the longitudinal strain distribution over the depth of the wall at centre span, the strain in the prestressing rod, the location of the rod in the hollow core, and the deflection of the wall were monitored (see Figure 1). Longitudinal strains across the joints where failure was likely to occur were monitored to detect the cracking load. From these readings the neutral axis location, the cracking load, the wall curvature, and the conditions of the prestressing rod could be monitored throughout each test.

EXPERIMENTAL RESULTS

A summary of the cracking and ultimate moments is given in Table 1. As for conventional reinforced concrete theory, under–reinforced failure (U/R) was assumed to occur when the reinforcement yielded before the masonry crushed; over–reinforced failure (O/R) occurred when the steel was below yield when the masonry crushed; and balanced failure (BAL) occurred when the steel yielded as the masonry failed.

Typical moment–central deflection curves for the "flexural" specimens with the three different arrangements of prestressing steel (grouted; guided and ungrouted; and unguided and ungrouted) are shown in Figures 2, 3 and 4. Although the behaviour

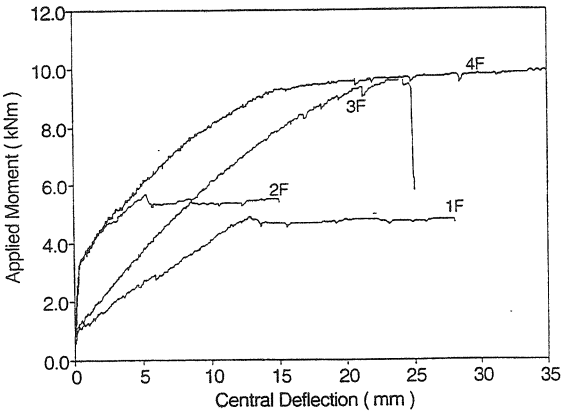

Figure 2. Flexural Behaviour of Grouted Walls

differs in each case because of the presence of grout or prestressing guides, it is significant to note the degree of ductility exhibited by all the panels. Even when over–reinforced the "shear" specimens exhibited similar flexural behaviour. Despite the fact that the arrangement of the loading was chosen to maximise the shear force on the section and induce a shear failure, no shear failures eventuated, with all walls failing in bending in a manner similar to the "flexure" specimens (see Table 1). It is apparent that shear effects will not be critical for prestressed hollow clay masonry walling with normal span/depth ratios.

Grouted Walls

For the grouted walls (Figure 2), a change in slope occurred in the moment–deflection curves at levels corresponding to the cracking load and this curve reached a plateau as the steel yielded or masonry failure occurred. The cracking loads for each wall were consistent with the level of prestress. Once initial cracking had occurred, the steel strains began to increase, and the rod size and properties then became significant, with a higher ultimate moment being achieved for the larger rod (see Figure 2). As the load increased in the post–cracking range, more cracks appeared in the joints along the length of the wall, with numerous joints being affected. The walls with the Y16 rod exhibited an under–reinforced failure and failed by steel yielding followed by large rotations at the point of failure, with final secondary crushing of the masonry occurring on the compression face. The walls with the TL20 rod were at or just below the point of balanced failure. At ultimate load the rod had begun to yield, but at the same time masonry spalling and mortar joint cracking was occurring. Both walls failed suddenly by the formation of a crack in the face–shell along the length of the wall adjacent to the grouted cavity, probably due to the difference in stiffness between the grouted and ungrouted cores. The four "shear" specimens behaved in a similar manner with under–reinforced failure in some cases, and more sudden over–reinforced failure in others (see Table 1). For the "shear" specimens the zone of peak moment was under the offset point load and the flexural failure occurred in this region.

Guided Walls

The behaviour of the guided "flexure" specimens is summarised in Figure 3. As the applied load was increased and the wall deflected, the steel rod moved towards the

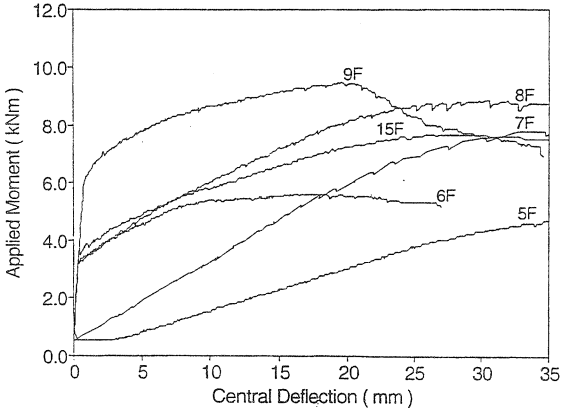

Figure 3. Flexural Behaviour of Guided Walls

compression face until the movement was restrained by the guides. The walls then cracked, and with further loading these cracks became visible. The cracking in this case was more localised than for the equivalent grouted cases, and the mortar joint at which most of the cracking and rotation occurred was between rather than at the guide locations. Once cracking occurred, the strain in the rod then began to increase until final failure. Walls 5F and 6F with the Y16 rod exhibited under–reinforced failure with the rod yielding first followed by mortar joint crushing (the bulk of the rotation was confined to one joint). By contrast the walls with the TL20 rod exhibited over–reinforced or balanced failures with the masonry failing in compression at the same time or before the yielding of the rod. The behaviour of the three "shear" specimens was similar with under–reinforced or over–reinforced behaviour being exhibited (see Table 1).

It is apparent from the curves in Figure 3 that the prestress levels control the cracking load, and the area of reinforcement in the section controls the ultimate strength of the prestressed wall. The cracked stiffness of the grouted wall was greater than that of the corresponding guided wall (Figures 2 and 3). This is because the elongation of the rod occurs over its full length for the guided wall and is more localised for the grouted wall. From the curves for the over–reinforced or balanced sections represented by 7F, 8F and 9F it can be seen that the prestress level affects the ultimate strength of the section with the ultimate strength increasing with prestress level. This effect, though not marked, is probably due to the lower rotations that occur in the failed joint when higher levels of effective prestress are present.

Unguided Walls

The effect of lack of restraint of the prestressing rods was significant, particularly with regard to the ultimate strength limit state. Up until cracking the behaviour of the guided and unguided cases was the same, with the cracking moments all being similar. However the cracked behaviour was affected by the movement of the rod in the core. As the cracked section deflected, the distance between the compression face of the wall and the steel decreased significantly. In the limit, for very large deflections, the rod actually came in contact with the compression face. This movement of the rod within the core reduced the lever arm between the compressive and tensile resultants of the cross section with an accompanying reduction in the moment of resistance. Failure was quite local, with the

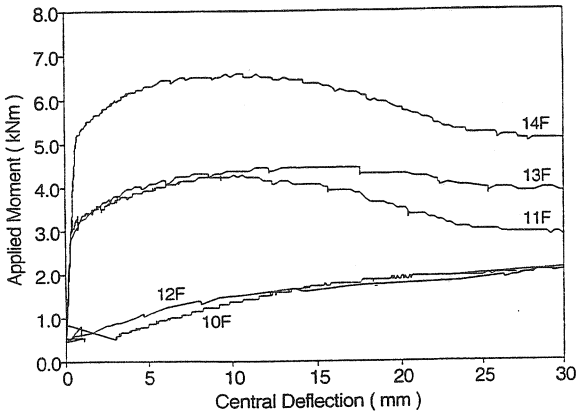

Figure 4. Flexural Behaviour of Unguided Walls

large deflection being accompanied by large rotations in the region of one cracked joint. This was accompanied by progressive compression failure at the corresponding location on the compression face. This behaviour was typical for both the "flexure" and "shear" specimens. The response of each of the specimens to out of plane loading is shown in Figure 4. For all the tests only a limited number of joints cracked (between one and three) and all subsequent rotation and distress was confined to one of these cracked joints.

As can be seen from Figure 4 the cracking moment depended upon the level of prestress with the values being consistent with those obtained from the other tests (see Table 1). After cracking the movement of the steel rod towards the compression face reduced the internal lever arm resulting in a lower ultimate moment than for the grouted or guided cases. All the "flexure" and "shear" specimens exhibited ductile behaviour regardless of whether they were under– or over–reinforced. In the over–reinforced cases the steel remained elastic and local compression failure occurred in the masonry (largely confined to the mortar joints). This local joint failure was accompanied by large local rotations and wall deflections. This apparent ductility (resulting from mortar crushing rather than steel yielding) would not necessarily be as pronounced in masonry where the strength of the hollow units was similar to the strength of the mortar. In this case the zone of compression failure could be more widespread.

Summary of Experimental Behaviour

The tests confirmed that, as for prestressed concrete, the level of prestress has a direct influence on the serviceability behaviour of the masonry, in particular the cracking moment. The ultimate behaviour is governed by the performance of the reinforced section since at this stage the prestress has been overcome and the masonry has cracked. Factors such as steel proportion, the presence of grout, and the degree of transverse restraint of the steel in the cores of the hollow masonry all affect the ultimate behaviour and must be considered. In contrast to reinforced and prestressed concrete, even over–reinforced sections exhibited ductile behaviour due to the progressive local crushing that took place in the mortar joints. Although it is desirable to achieve under–reinforced failure by limiting the steel proportion, in this case it may not be as critical.

ANALYTICAL MODELLING OF FLEXURAL BEHAVIOUR

In designing prestressed masonry realistic analytical models are required for both the serviceability and ultimate strength limit states. In both cases appropriate load factors and capacity reduction factors are applied to the basic strength equations. In this analysis both the load and capacity reduction factors are taken as unity.

Serviceability Limit State
The level of prestress can be used to control the load at which cracking occurs. Assuming elastic behaviour the cracking moment of a cross section is given by

$$M_{cr} = \frac{\left(\sigma_{me} + f'_{mt}\right) I_g}{y_t} \qquad [1]$$

where

σ_{me} = effective prestress in the masonry (including appropriate corrections for losses)
f'_{mt} = flexural bond strength of the masonry
I_g = second moment of area of the cross section
y_t = distance from the centroid of the section to the extreme tensile fibre

The cracking moments for each of the "flexure" and "shear" walls were calculated using the mean value of bond strength of 0.21 MPa (obtained from bond wrench testing), the effective prestress levels from Table 1, and section properties based on the nominal face–shell bedded cross section including the transformed area of the steel in the grouted cases.

A comparison of the predicted and observed cracking moments for all the walls tested (excluding those with zero prestress) indicated that equation [1] predicts the cracking moment with reasonable accuracy. Better agreement was obtained for the "flexure" tests than the "shear" tests, probably because the "flexure" test produced a zone of constant bending moment in the monitored region. (The ratio of the predicted to observed cracking moments was 0.92 for the "flexure" tests and 0.80 for the "shear" tests). One of the reasons for the variation in the predicted cracking moments was the high variability of the flexural bond strength of the masonry. If the actual bond strength in each case had been available, a better correlation would probably have been achieved. (The cracking moments for the unstressed walls indicated that the bond strength and/or the second moment of area of the test specimens were often larger than the assumed values). The variation in values of bond strength will become less important as the level of prestress increases, since it becomes a smaller fraction of the tensile capacity of the section. The normal assumption in design is to take the flexural bond strength as zero. This will always lead to a conservative prediction of the cracking load, with the effect of this assumption also becoming less pronounced as the level of prestress increases.

Strength Limit State
The ultimate strength of the section is governed by the cracked section behaviour. This behaviour will be influenced by the steel proportion of the section, whether the steel is bonded or unbonded, and the degree of transverse restraint of the steel in the hollow cores. The steel stress at ultimate, σ_{pu}, must also be known or estimated. If the section is under–reinforced and the prestressing steel has a well defined yield stress, then the steel stress will be known. In other cases the steel stress must be obtained either from first

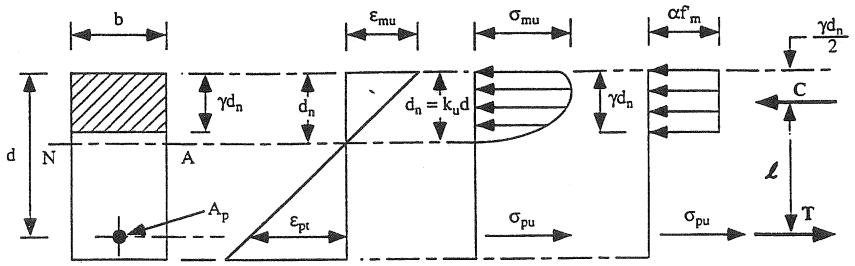

Figure 5. Ultimate Behaviour of a Prestressed Section

principles or by an empirical approach. Figure 5 shows the typical and assumed stresses on a prestressed masonry section at ultimate. As for prestressed concrete an equivalent rectangular compression stress block is substituted for the actual parabolic distribution. The ultimate moment M_u is then given by

$$M_u = T \cdot \ell = C \cdot \ell \qquad [2]$$

where T and C are the tensile and compressive resultants on the section and ℓ is the lever arm between the two forces. Following normal reinforced concrete theory, by equating C and T, the neutral axis depth d_n is given by

$$d_n = \frac{\sigma_{pu} A_p}{\alpha f'_m b \gamma}$$

In prestressed masonry γ, the parameter defining the depth of the rectangular stress block, is usually taken as 1 (Phipps, 1993). Substituting for d_n in equation (2) and expanding yields

$$M_u = \sigma_{pu} A_p \left(d - \frac{\sigma_{pu} A_p}{2\alpha f'_m b} \right) \qquad [3]$$

In the experiments σ_{pu} was measured directly as were the variations in effective depth for the unbonded cases. In design σ_{pu} and d must be estimated. The only other unknown in equation [3] is α, one of the parameters defining the rectangular stress block which in turn may be influenced by the method used to determine the masonry compressive strength f'_m. (If a small prism specimen is used there will be a size effect which would need to be considered to relate this strength to the strength of the masonry in the actual wall). In this investigation f'_m was obtained from tests on four high prisms made from single face–

Table 2. Ratio of the Predicted and Experimental Ultimate Moments

Method	$M_{u(Pred)}/M_{u(Exp)}$	
	Mean	Coefficient of Variation
α = 0.85		
a. "Flexure"	0.96	15.7%
b. "Shear"	0.96	10.7%
α = 1.0		
a. "Flexure"	0.99	15.6%
b. "Shear"	0.99	11.2%

shells cut from larger units. This test was aimed at simulating the behaviour of the compressive zone of the section at ultimate when the face–shell on the tensile side of the neutral axis is cracked and there is a reasonably uniform distribution of compressive stress on the other face–shell.

Comparison of Predicted and Observed Ultimate Moments With a Measured Value of σ_{pu}

Two sets of comparisons were made with assumed values of α of 0.85 and 1.0. Comparisons of the predicted and observed ultimate moments for all the bonded and unbonded cases are given in Table 2. It can be seen that good agreement was obtained with a marginally better correlation with α = 1.0. The results also confirmed the applicability of equation [3] indicating that the normal prestressed concrete approach is appropriate for predicting the ultimate moment of a section.

Design Approach – Prediction of σ_{pu} and M_u

In design the stress in the steel at ultimate must be estimated to determine the ultimate moment. A full review of available techniques has been produced recently (Graham, 1995). A brief treatment follows here.

Bonded Construction

If the steel is bonded in a core by grouting, strain compatibility will apply and the usual strain compatibility methods from prestressed concrete theory can be used to determine the ultimate steel stress. An iterative procedure is used to determine the ultimate steel strain (and stress) by considering the sum of the strains due to the effective prestress, the strain required at the level of the tendon to offset the effective prestress, and the tensile strain induced in the steel by additional flexure as a cracked section.

The experimental values for the grouted cases were compared to those predicted by the above technique. The mean ratio of the predicted to the observed moment for all stressing levels was 1.03 with a coefficient of variation of 11.9%, indicating that the method provides an accurate means of predicting ultimate behaviour.

Unbonded Construction

If the section is unbonded the strain in the steel will be an average value based on its full unbonded length, and a semi empirical method is required to determine σ_{pu}. This problem was originally investigated by Pannel in relation to prestressed concrete (Pannel, 1969). Pannel assumed that all the deformation in the concrete in the compression zone was confined to a local region at the moment hinge with a plastic length equal to $\psi \cdot d_n$.

With α and γ taken as 1, this yields the expression

$$\sigma_{pu} = \sigma_{pe} + \frac{\psi \cdot \varepsilon_{mu} E_p d}{L}\left(1 - \frac{\sigma_{pu} A_p}{f'_m b d}\right) \qquad [4]$$

where

ε_{mu} = the ultimate strain in the masonry
A_p = the cross sectional area
E_p = the elastic modulus of the prestressing rod
L = the unbonded length (usually the span length)

This equation can be simplified by an approximation for the σ_{pu} term on the right hand side, since the expression is relatively insensitive to the value of the last term. A common approximation is to assume a value of 70%–85% of the ultimate strength of the steel. For brick masonry a value of 70% has been suggested (Phipps, 1993).

Recent British work (Phipps, 1993) has proposed an expression based on Pannels theory and this has been adopted in the British Code. If the material safety factor for masonry of 2 is removed the suggested relationship is

$$\sigma_{pu} = \sigma_{pe} + \frac{700\, d}{L}\left(1 - \frac{0.7\, \sigma_p A_p}{f'_m b d}\right) \qquad [5]$$

A comparison of the observed ultimate moments and those predicted by equation [3] using the Phipp's expression for σ_{pu} is given in Figure 6. It can be seen that the Phipp's approximation consistently yields a conservative prediction of the ultimate moment with the degree of conservatism reducing with increased stress level. Equation [5] therefore appears to be a conservative design approach.

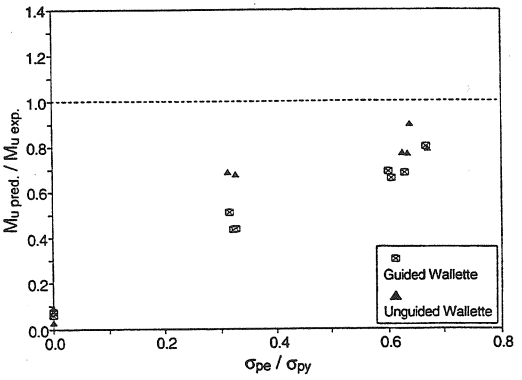

Figure 6. Comparison of Predicted and Observed Ultimate Moments (Unbonded Construction)

CONCLUSIONS

An experimental and analytical investigation of the flexural behaviour of post–tensioned hollow masonry has been described. The significance of prestress level, reinforcement ratio and prestressing rod restraint conditions have been investigated. Although replicates of each of the tests have not been performed the trends are clear. As for prestressed concrete the level of prestress has a direct influence on the serviceability behaviour, in particular the cracking moment. Conventional elastic analysis can be used to determine the uncracked capacity. The degree of restraint of the rod in the core of the hollow units is not critical at this stage. However it does have a marked influence on the ultimate behaviour, since the rod is free to move in the cavity and geometric effects become significant. The capacity of the wall is then reduced, and the failure mode can change from under–reinforced to over–reinforced. It is therefore desirable to restrain the rod within the core of the hollow unit either by grouting the core or by using inserts to hold the rod in place. If the cores of the hollow units are grouted so that strain compatibility can be achieved between the steel and the grout, the ultimate moment can be accurately predicted using normal strain compatibility methods. If the prestressing rods are unbonded, a semi empirical approach must be used to determine the ultimate capacity of the section. The relationship proposed by Phipps yields a conservative estimate of the ultimate strength in this case. It also appears from the tests that for normal span/depth ratios, hollow masonry walls subjected to lateral loading will always fail in flexure, with shear effects being secondary.

ACKNOWLEDGMENTS

The financial support of the Wide Bay Brickworks and the Rod and Bar Products Division of BHP Steel is gratefully acknowledged, as is the assistance of the CBPI and laboratory staff of the Department of Civil Engineering and Surveying.

REFERENCES

Graham, K.J., (1995), The Flexural Behaviour of Prestressed Hollow Clay Masonry, Master of Engineering Thesis, The University of Newcastle, Australia.

Hendry, A.W., (1991), Reinforced and Prestressed Masonry, Longman Scientific and Technical, John Wiley and Sons, 1991, pp. 125–159 and 78–98.

Graham, K.J. and Page, A.W., (1994), An Experimental Study of Flexural Behaviour of Post Tensioned Hollow Clay Masonry, Proceedings 10th IBMAC, Calgary, July, pp. 639–648.

Pannel, F.N., (1969), The Ultimate Moment of Resistance of Unbonded Prestressed Concrete Beams, Magazine of Concrete Research, March, Vol. 21, No. 6, pp. 43–54.

Phipps, M.E., (1993), The Principles of Post Tensioned Masonry Design, Proceedings 6th North American Masonry Conference, Phil., June, pp. 621–632.

Schultz, A.E. and Scolforo, M.J., (1991), An Overview of Prestressed Masonry, The Masonry Society Journal, Vol. 10, No. 1, August, pp. 6–21.

Schultz, A.W. and Scolforo, M.J., (1992), Engineering Design Provisions for Prestressed Masonry – Part 1: Masonry Stresses, The Masonry Society Journal, Vol. 10, No. 2, February, pp. 29–47.

Schultz, A.W. and Scolforo, M.J., (1992), Engineering Design Provisions for Prestressed Masonry – Part 2: Steel Stresses and Other Considerations, The Masonry Society Journal, Vol. 10, No. 2, February, pp. 48–64.